Transfer Functions and Current Distribution Algorithm for the Calculation of Radiated Emissions of Automotive Components

D. Schneider[1*], M. Böttcher[1], B. Schoch, S. Hurst[1], S. Tenbohlen[1], W. Köhler[1]
[1]Institute of Power Transmission and High Voltage Technology (IEH)
University of Stuttgart, Germany
[*]daniel.schneider@ieh.uni-stuttgart.de

***Abstract*— Radiated emission testing of electric components, modules and systems is mandatory. Such tests are performed in absorber-lined shielded enclosures during the development process. Due to strict time schedules, limited access to EMC measurement facilities and cost reasons, alternative methods are needed. This contribution presents an approach for a pre-compliance test method for radiated emissions of automotive components. It is adapted to gain measurement results according to the CISPR 25 standard. The later operation site of this pre-compliance test method is the developer's laboratory setup. For obtaining the radiated field strength of an tested device common mode currents on the cable harness are measured. As the current distribution along a harness is needed for accurate calculation in higher frequency ranges, an algorithm is presented retrieving the current distribution out of current probe measurements. Those current distributions in combination with multiple transfer functions lead to a calculation of the electrical field strength. Transfer functions represent the correlation between common mode current in the defined test setup environment and their electric field strengths. The methodology of transfer functions using a vector network analyzer will be explained. The transfer functions for a single segment and multiple segments will be verified, compared, and applied to a realistic test setup.**

Keywords*— *CISPR 25; EMC; Pre-Compliance Test; Radiated Emission; Transfer Functions

I. INTRODUCTION

Electric automotive components require radiated emission tests according to CISPR 25 [1]. Those measurements are performed in absorber-lined shielded enclosures (ALSE). The test setup is placed on a grounded metallic table bonded to the enclosure. It consists of the equipment under test (EUT), a cable harness connecting the EUT to a load or optionally to line impedance stabilization networks (LISNs), and a power supply. The measurement antenna is situated one meter in front of the table.

EMC engineering in parallel to the development process is very challenging due to strict time schedules and limited access to EMC measurement facilities. Early knowledge of the EMC performance is important regarding suitable countermeasures. Hence, pre-compliance test methods are desired. They should be fast and applicable on-site. Methods for predicting radiated emissions from simple setups mainly use the field domination of common mode (CM) currents on the cable harness [2]. This permits current probe measurements around an entire cable bundle as the basis for pre-compliance calculation methods.

Analytical methods rely on Hertzian dipoles, which represent cable bundles and take parts of the geometry of the test setup into account [3], [4], [5], [6]. Disadvantage of those approaches is the unconsidered near field coupling of the antenna with the setup, as well as the antenna factor. Further, the ALSE characteristic is not included. A hybrid approach employing multiple measured transfer functions (TF) is presented in [7]. This approach uses TFs of cable harness segments along the harness' position. Therefore, the method includes the entire measurement environment, like anechoic chamber characteristics, near field coupling of the measurement antenna with the setup and the geometrical conditions. Reproducing those aspects into a numerical or analytical model is difficult, time consuming and not constructive. A single segment approach of the TF method using scattering parameter measurements with a vector network analyzer (VNA) is analyzed in [8]. This single segment approach is limited to similar setups due to changing current distributions on cable harnesses for different setups and EUTs. Hence, an advanced version of [7] the multiple segments transfer functions (MSTF) including a current distribution algorithm without the need of extra phase information will be presented. A comparison between the MSTF and the single segment TF will be performed by verification measurements and furthermore by a realistic wiper motor setup.

II. CURRENT DISTRIBUTION ALGORITHM

The knowledge of the current distribution along a wire bundle is essential for a correct calculation of the radiated electric field. The CM current envelopes for each frequency can be received by multiple current probe measurements along a harness with an EMI test receiver in peak mode. Those measured envelopes do not have to be the current distributions for the corresponding peak value of the electric field strength measured by an antenna. This is only the case if there is a standing wave on the wire bundle. Envelopes can be used for frequencies where the cable is electrically small. Mainly, there are propagating composite waves on the harness. They consist of forward and reflected waves and have a current standing wave ratio (CSWR) smaller than infinite. For this reason, an infinite number of distribution curves for each frequency exist.

Fig. 1 shows a calculated and theoretical series of 36 composite waves for 200 MHz, their maximum and minimum envelopes, and the composite $I_{composite,\ max\ SI}$ with the maximum surface integral. In this example the curves are equally spaced with a phase shift of 2π/10. The length of the assumed cable is 1.8 m, the CSWR equals two, and cable attenuation is 0 dB.

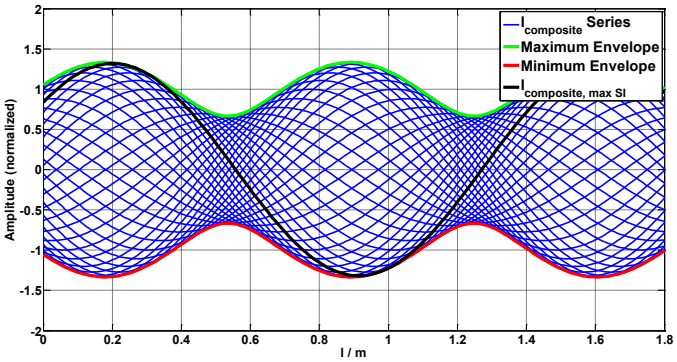

Fig. 1: Calculated current distribution at 200 MHz for a 1.8 m long cable

Composite curve series can be retrieved out of measured envelopes. This is suitable as long as the cable length is bigger than half the wave length of the frequency of interest. In this case, at least one maximum a_{max} and one minimum a_{min} of the envelope curve per frequency are contained if there are sufficient measurement points along a harness. Those values are used to calculate the amplitudes $a_r(f)$ of the reflected waves (1) and $a_f(f)$ of the forward waves (2). By knowledge of the maximum's position $x_{a_{max}}(f)$ the forward waves $fwd(f)$ and the reflected waves $ref(f)$ can be calculated according to (3) and (4) for different phasings. For being appropriate for the MSTF the additional phase shifts $\varphi_{E,i}$, explained in section III, of the electric field fractions have to be inserted. Superposition of the forward and reflected waves lead to the current distributions $I_{CDA,z}(f)$ (5):

$$a_r(f) = 0.5\,(a_{max}(f) - a_{min}(f)) \quad (1)$$

$$a_f(f) = a_{max}(f) - a_r(f) \quad (2)$$

$$fwd(f,z) = a_f(f)\,\sin\left(\beta(f)\,x - \beta(f)\,x_{a_{max}}(f) + \frac{\pi}{2} - 2\pi\,z - \varphi_{E,i}(f)\right) e^{-\alpha x} \quad (3)$$

$$ref(f,z) = a_r(f)\,\sin\left(\beta(f)\,x - \beta(f)\,x_{a_{max}}(f) + \frac{\pi}{2} + 2\pi\,z + \varphi_{E,i}(f)\right) e^{-\alpha x} \quad (4)$$

$$I_{CDA}(f,z) = fwd(f,z) + ref(f,z) \quad (5)$$

with the phase constant $\beta(f)$, the position array x along the cable bundle, phase shift coefficient $z \in [0,1]$, and the attenuation coefficient $\alpha(f)$.

For the result in Fig. 2, a 1.8 m long two-wire cable harness is excited by a VNA. Nine current probe measurements are taken each 0.2 m, starting at the sample position 0.1 m. Out of those measurements the envelopes for each available frequency step are generated. The composite series is calculated by (1) to (5) with $\varphi_{E,i}$ set to zero showing the applicability of the presented algorithm reproducing the current along a cable. In Fig. 2 the measured envelopes and one calculated current distribution $I_{composite,\ max\ SI}$ with maximum surface integral for 200 MHz are plotted.

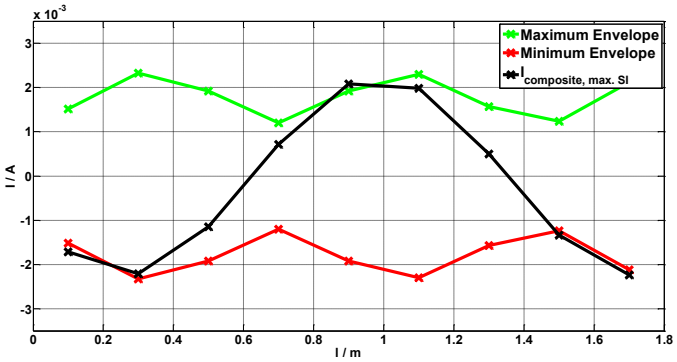

Fig. 2: Current distribution at 200 MHz for a 1.8 m two-wire cable

The presented calculation procedure is still a proper approximation for cable lengths shorter than half the wave length of the frequency of interest. This does not count in regions of cable resonances. Fig. 3 shows $I_{composite,\ max\ SI}$ with maximum surface integral compared to the envelopes for 30 MHz with $\varphi_{E,i}$ set to zero.

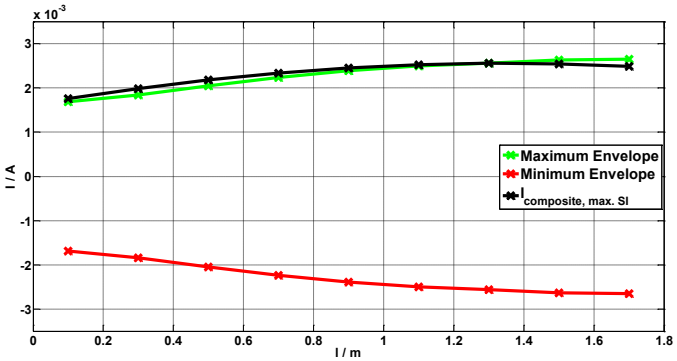

Fig. 3: Current distribution at 30 MHz for a 1.8 m two-wire cable

One important question for field calculation is: Which current distribution $I_{CDA}(f,z)$ leads to the peak value of the electric field strength? The composite wave $I_{composite,\ max\ SI}(f)$ with the highest surface integral is responsible for the maximum field value in the far field. This is not valid under near field conditions due to the influence of phase shift $\varphi_{E,i}$. For gaining the maximum field strength, the electric field out of each current distribution $I_{CDA}(f,z)$ has to be calculated and the maximum value for each frequency has to be determined.

III. Methodology of Transfer Functions

The TF method uses the correlation between CM currents on a cable bundle and its radiated electrical field. This correlation can be obtained by a measurement procedure [7], [8]. Differential mode currents are not considered. Their contribution to the entire field strength is neglected because of the closely spaced wires in a harness [2], [8]. A TF contains properties of the test setup like near field coupling of the antenna with the setup, anechoic chamber characteristics, and the geometrical conditions of the entire setup. This can be achieved by the use of a current probe measurement on a harness detecting the CM current $\hat{I}_{CM}(f)$ and by an antenna measuring the electric field strength $\hat{E}(f)$ in an ALSE. The theoretical TF in the frequency domain for a single segment representing an entire cable harness, see Fig. 4, is defined by:

$$TF(f) = \frac{\hat{E}(f)}{\hat{I}_{CM}(f)} \tag{6}$$

According to [8] a single segment TF can be generated using a VNA. Therefore, three ports of a VNA are connected to the generation setup as depicted in Fig. 4 leading to the 3-port version:

$$TF(f) = \left|\frac{S_{31}(f)}{S_{21}(f)}\right| \cdot AF(f) \cdot Z_T(f) \tag{7}$$

with the scattering parameters $S_{31}(f)$ and $S_{21}(f)$, the antenna factor $AF(f)$ and the transimpedance $Z_T(f)$ of the current probe. Having only a 2-port VNA, the current probe measurement and the antenna measurement respectively, can be carried out successively. This leads to a 2-port version.

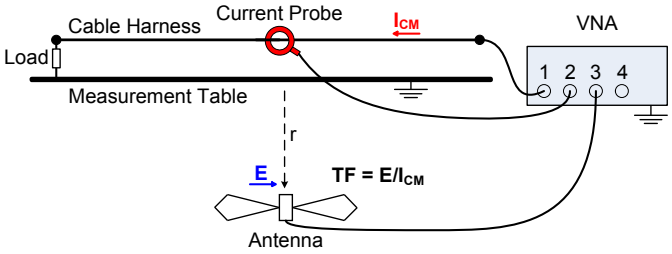

Fig. 4: Generation setup for a single segment TF

A prediction of the radiated electric field strength can be made measuring the CM current on a similar setup with the EUT of interest. This setup is located at the developer's laboratory. The EUT is connected to the cable harness instead of the VNA. The CM current $\hat{I}_{EUT}(f)$ measured on the same position as during the TF generation with an EMI test receiver and the according $TF(f)$ lead to the radiated emission $E_{pre}(f)$, representing the pre-compliance result:

$$E_{pre}(f) = TF(f) \cdot \hat{I}_{EUT}(f) \tag{8}$$

A single segment TF includes the CM current distribution on the used cable harness excited by a VNA. With the single segment approach an identical current distribution for the EUT setup and the TF generation setup is needed to be accurate. Due to the change from a VNA in an ALSE to an arbitrary EUT in a laboratory environment changed parasitic capacitances and load impedances occur. Hence, the pre-compliance result can be incorrect. A more flexible solution is presented in [7]. Here, multiple TFs representing a cable harness are generated. An advanced approach is shown in [9] and will be discussed and investigated further in the following.

For the MSTF a cable harness is divided into multiple segments. For each ith segment and its position a $TF_i(f)$ has to be generated according to (7). Fig. 5 illustrates the procedure. Additionally, each segment has a distance r_i to the measurement antenna causing a phase shift $\varphi_{E,i}(f)$. All scattering parameter sets of the single TFs include this phase information, which is represented by the angle of $S_{31,i}(f)$:

$$\varphi_{E,i}(f) = \measuredangle S_{31,i}(f) \tag{9}$$

The phase shift $\varphi_{I,i}(f)$ of the current between the segments has to be known and taken into account. This can either be considered by VNA measurements presented in [9] or by the use of the current distribution algorithm presented in section II. This makes measurements of phase information for the current unnecessary.

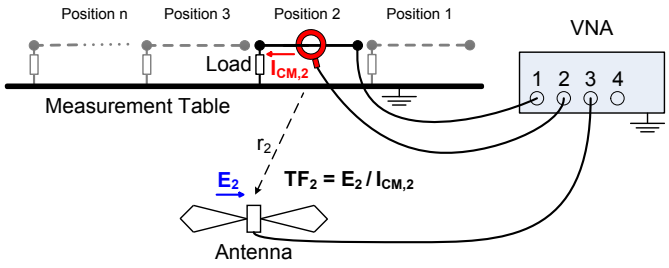

Fig. 5: Setup for the generation of multiple transfer functions

The calculation of the electric field can be performed with the information of the single segments in combination with current probe measurements $\hat{I}_{EUT,i}(f)$ using an EMI test receiver in peak mode on the EUT's test setup. There are two calculation methods. One employing $\hat{I}_{EUT,i}(f)$ and determined phase shift $\varphi_{I,i}(f)$ and one applying the mentioned current distribution algorithm leading to the currents $I_{CDA,i}(f,z)$. The currents and the $TF_i(f)$ lead to the calculated electrical field strengths $E_{pre,i}(f)$ and $E_{pre,CDA}(f)$ by superposition of each segment's field fraction according to (10) and (11). Fig. 6 illustrates the superposition procedure.

$$E_{pre,\hat{I}}(f) = \left|\sum_{i=1}^{n} TF_i \cdot \hat{I}_{EUT,i}(f) e^{j(\varphi_{I,i}(f)+\varphi_{E,i}(f))}\right| \tag{10}$$

$$E_{pre,CDA}(f) = max\left[\sum_{i=1}^{n} TF_i \cdot I_{CDA,i}(f,z)\right] \forall z \tag{11}$$

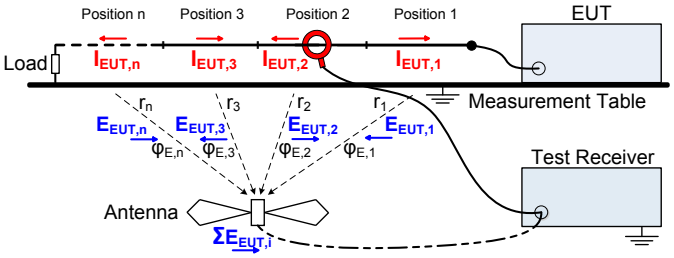

Fig. 6: Calculation of the electric field strength by superposition of each segment's field fraction

It is recommended to use the 2-port version for the $TF_i(f)$ generation due to the feedback of the current probe on the radiated emission of a segment [10]. Therefore, the current probe shall not be around the harness of a segment during the antenna measurement.

IV. Harness Segmentation

In the following measurement setups a 1.8 m long two-wire harness will be used. For representing the entire harness up to a frequency of 200 MHz the number of needed segments has to be chosen. The length of one segment should be in the range of λ/10 - λ/6 of 200 MHz. This is required to have an electrically short segment. Hence constant current amplitudes along a segment exist. Due to the cable configuration the phase velocity is around $2.844 \cdot 10^8$ m/s. Therefore, the length of a segment should be in between 142 and 237 mm. This leads to a number of segments needed between 7 and 13. By use of an analytic model [5] representing the CISPR 25 setup

and a calculated current distribution, the error in the electric field strength calculation depending on the segmentation degree will be investigated. The horizontal field component $E_{calc,\ 180\ Seg}$ is computed out of 180 segments as reference. For comparison, the field is computed on base of 9 segments. Fig. 7 shows the result of the calculations. Up to 188 MHz the error between the reference curve $E_{calc,\ 180\ Seg}$ and $E_{calc,\ 9\ Seg}$ is equal or smaller than 0.1 dB. The highest deviation of 0.3 dB occurs at 200 MHz. Those deviations can be neglected in means of a pre-compliance method. Having a 1.8 m harness, 9 segments are chosen for measurements, giving segment lengths of 200 mm.

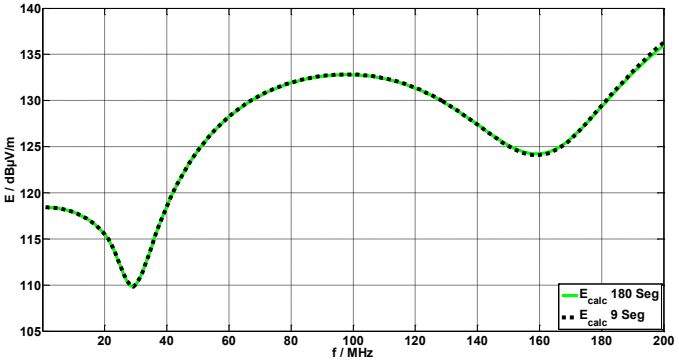

Fig. 7: Comparison of horizontal electric field strength $E_{calc\ 180\ Seg}$ to field strength calculated out of 9 segments using an analytic model

A segment for the MSTF generation consists of a part of the cable harness used for the EUT of interest. This contribution focuses on a two-wire harness for plus and minus power supply, as used in the automotive area. Hence, two LISNs have to be considered. Each wire has a simplified LISN replication as load. Fig. 8 shows a schematic of a segment and Fig. 9 the employed segment consisting of a metallic base plate, two wires, a coupling printed circuit board (PCB), a termination PCB including the LISN replications, and the attached current probe. The values of the components are: $C_1 = 0.1$ µF, $C_2 = 1$ µF, R = 50 Ω, L = 5 µH. The used coupling PCB allows a CM excitation of both wires.

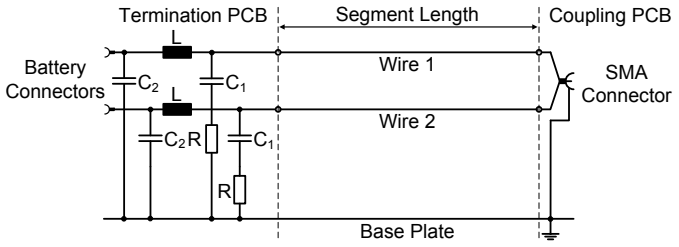

Fig. 8: Schematic of a segment for the transfer function generation

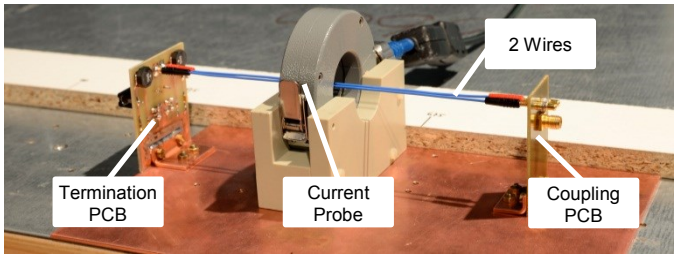

Fig. 9: Two-wire segment for the transfer function generation

V. Verification Measurement

Calculated and measured electric field strength have to be compared using the same noise source to verify the single segment TF and the MSTF. The test setup consists of a 1.8 m long two-wire harness and is located 50 mm above a ground plane. It is terminated with the same termination PCB described in section IV representing two LISNs. The noise source for the verification setup is a VNA exciting the cable harness with the same settings as during the TF generation. Fig. 10 shows the verification setup. Variations in the ground potential of the VNA and EMI test receiver, due to bad ground connections, can affect the accuracy of the method. Because of the performance of the available ALSE, the VNA and EMI test receiver are located on the measurement table as one common ground plane reducing deviations. Single segment TF and MSTF data of this setup is gained as described in section III. The CM currents are measured using an EMI test receiver at the same locations TFs are determined. The predicted electric field strength caused by the excited harness can be calculated by (8) for the single segment TF and by (10) or (11) for the MSTF. As reference, the electric field strength is measured using a monopole for the frequency range of 0.3 to 30 MHz, and with a biconical antenna in horizontal and vertical polarization for the frequency range of 30 to 200 MHz by an EMI test receiver. The caused noise floor of the EMI test receiver and the VNA is below the emission of the harness and does not affect the calculation result. Currents and electric field strength are measured by an EMI test receiver in peak mode. Measured data is always above the noise floor.

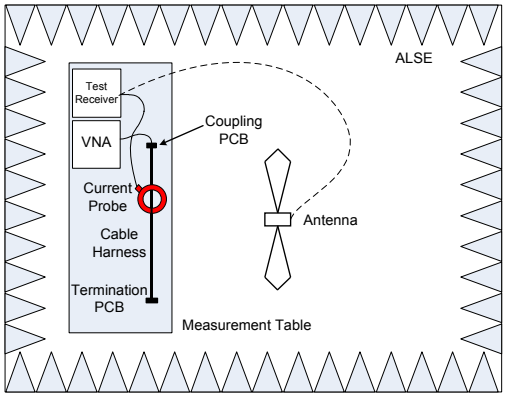

Fig. 10: Graph of the test setup for verification purposes in an ALSE

Fig. 11 shows the verification result for the frequency range of 0.3 to 30 MHz. The single segment result $E_{pre,\ VNA,\ 1\ Seg}$ replicates the reference measurement $E_{meas,\ VNA}$ with maximum deviation of less than 1.5 dB. The two MSTF results $E_{pre,\ VNA,\ I_{CDA}}$ and $E_{pre,\ VNA,\ \hat{I}}$ reproduce the reference measurement $E_{meas,\ VNA}$ up to 5.5 MHz with an error of less than 2 dB. Between 5.5 and 30 MHz the maximum error for $E_{pre,\ VNA,\ I_{CDA}}$ and for $E_{pre,\ VNA,\ \hat{I}}$ is 9 dB.

Fig. 12 shows the verification result for the frequency range of 30 to 200 MHz in horizontal polarization. The single segment result $E_{pre,\ VNA,\ 1\ Seg}$ replicates the reference measurement $E_{meas,\ VNA}$ with a maximum deviation of 0.6 dB. The MSTF result $E_{pre,\ VNA,\ I_{CDA}}$ reproduces the reference

measurement $E_{meas,\ VNA}$ with a maximum error of around 10 dB, except the λ/2 resonance around 82 MHz which is not replicated. In this region the current distribution algorithm is not able to reproduce the current needed for an accurate field calculation. $E_{pre,\ VNA,\ \hat{I}}$ reproduces the reference measurement $E_{meas,\ VNA}$ with a maximum error of around 10 dB.

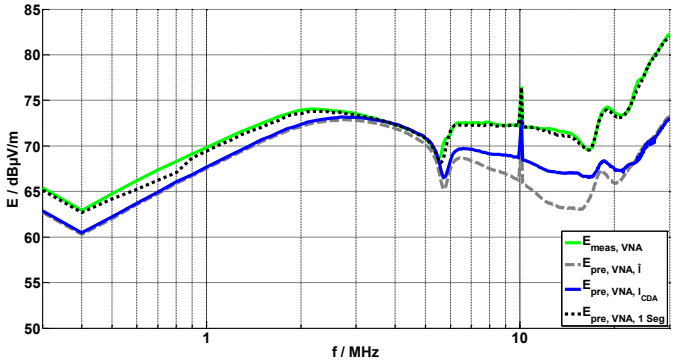

Fig. 11: Verification result in the range of 0.3 – 30 MHz

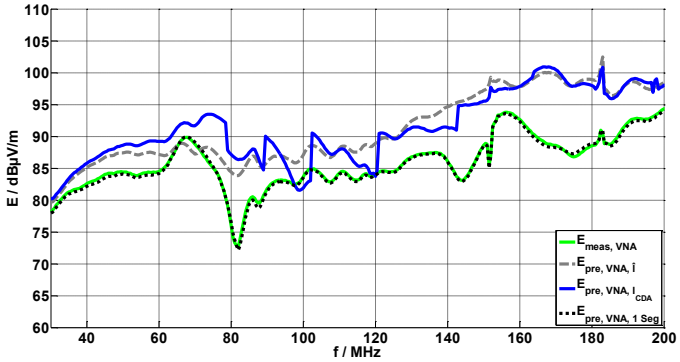

Fig. 12: Verification for horizontal polarization in the range of 30 - 200 MHz

Fig. 13 shows the verification result for the frequency range of 30 to 200 MHz in vertical polarization. The single segment result $E_{pre,\ VNA,\ 1\ Seg}$ replicates the reference measurement $E_{meas,\ VNA}$ with a maximum deviation of up to 4 dB. Both MSTF results $E_{pre,\ VNA,\ I_{CDA}}$ and $E_{pre,\ VNA,\ \hat{I}}$ have their maximum deviations around 45 MHz and around 193 MHz compared to $E_{meas,\ VNA}$. In between a maximum error of around 10 dB can be observed.

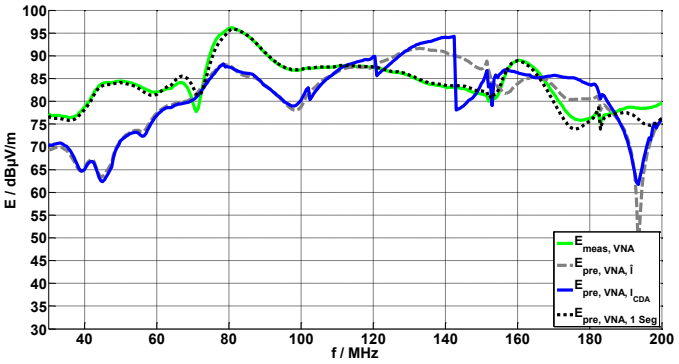

Fig. 13: Verification for vertical polarization in the range of 30 - 200 MHz

As a result, the prediction of the electric field using MSTFs including LISNs is proven in certain frequency ranges with adequate accuracy within ±10 dB. The proposed current distribution algorithm delivers comparable results without the need of current phase information. Deviations between field prediction and measurement are caused by multiple reasons. One reason could be the used termination PCB. In future work the impedances of the LISNs have to be transformed according to the transmission line theory to each location of the termination PCB of a segment instead of a fixed configuration. Further, the influence of the segment during the TF generation, imperfect termination impedances, geometrical and measurement uncertainties, as well as radiation, phase stability, and position of the measurement cables have to be considered as source of errors.

VI. Practical Example

To prove the applicability of the TF method an EUT is investigated. A wiper motor is used on the same test setup presented in section V. Additionally a 12 V battery is attached to the battery connectors of the termination PCB. The verified TFs are used for computing the electric field strength. The CM currents are measured at the same locations as before.

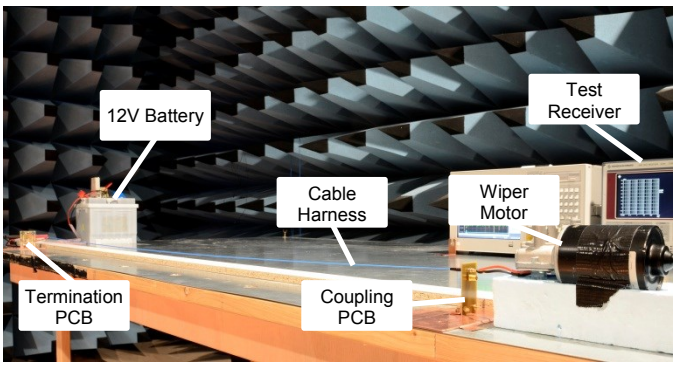

Fig. 14: Test setup for a wiper motor

The calculated electric field strength for the wiper motor in the frequency range of 0.3 to 30 MHz is compared to the reference measurement $E_{meas,\ Motor}$ in Fig. 15. As can be seen, the deviation between field measurement and prediction for the single segment calculation $E_{pre,\ Motor,\ 1\ Seg}$ is mostly below 5 dB up to 30 MHz. The 9 segments calculations $E_{pre,\ VNA,\ I_{CDA}}$ and $E_{pre,\ VNA,\ \hat{I}}$ deliver a good result up to 10 MHz with a maximum error of around 5 dB. All three types of calculation lead to a sufficient accuracy for a pre-compliance test result. Nevertheless, the one segment method is preferable due to less effort.

The result for the horizontal frequency range within 30 to 200 MHz is presented in Fig. 15. From 30 to 125 MHz $E_{pre,\ Motor,\ 1\ Seg}$, the single segment TF result, has a maximum deviation of around 5 dB, except at the resonance of 82 MHz. Above 125 MHz up to 25 dB of error occurs. The 9 segments calculation $E_{pre,\ VNA,\ \hat{I}}$ gives a satisfying performance beginning from 95 MHz with mainly less than 6 dB of deviation. In this frequency region it delivers better results than the single segment TF due to the considered current distribution. In between 140 to 160 MHz deviations of up to 15 dB occur. $E_{pre,\ VNA,\ I_{CDA}}$ is comparable but with higher noise offset. All results can be used as a pre-compliance result.

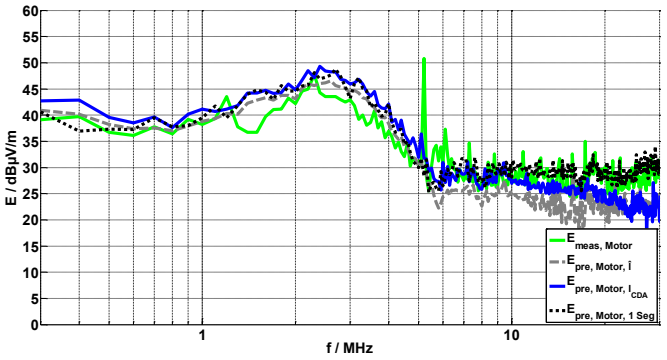

Fig. 15: Pre-compliance results for the wiper motor compared to the reference measurement $E_{meas,\ Motor}$ in the range of 0.3 – 30 MHz

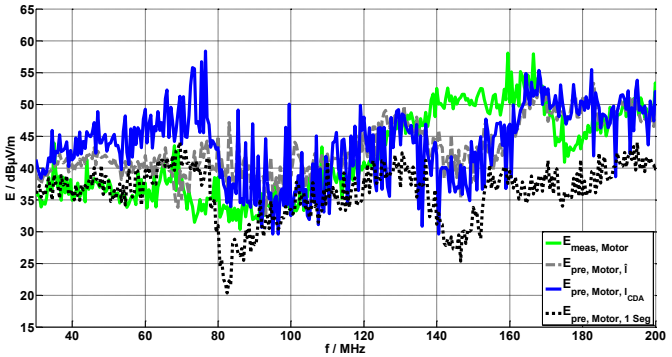

Fig. 16: Horizontal pre-compliance results for the wiper motor compared to the reference measurement $E_{meas,\ Motor}$ in the range of 30 – 200 MHz

Fig. 17 shows the result for vertical polarization in the range from 30 to 200 MHz. From 30 to 125 MHz $E_{pre,\ Motor,\ 1\ Seg}$, the single segment TF result, has a maximum deviation of around 5 dB. Above 125 MHz up to 20 dB of error occurs. The 9 segments calculations $E_{pre,\ VNA,\ Î}$ and $E_{pre,\ VNA,\ I_{CDA}}$ give a satisfying performance in between 60 to 120 MHz.

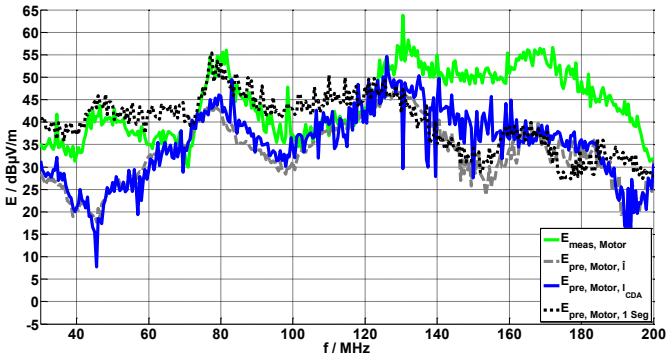

Fig. 17: Vertical pre-compliance results for the wiper motor compared to the reference measurement $E_{meas,\ Motor}$ in the range of 30 – 200 MHz

VII. Conclusion and Outlook

This paper presents a method for the prediction of radiated emissions according to the CISPR 25 standard for component tests. Current probe measurements on an EUT's cable harness in combination with a single segment TF or MSTF lead to a fast estimation of radiated emissions under the assumption of field dominating CM currents on a cable harness. This method can be applied to a developer's laboratory setup without having an ALSE allowing fast and easy pre-compliance measurements. The methodology and the verification of the TF method are explained. Current distribution retrieval as a basis for the calculation of higher frequencies without the need of extra phase information for the current is explained. A wiper motor is presented as use case. This realistic test setup shows the applicability of the single segment TF and the MSTF. The single segment TF delivers usable pre-compliance results from 0.3 up to 120 MHz. For higher frequencies the MSTF yield to better results for horizontal polarization, justifying the additional expense. A combination of both approaches will lead to the best result over the entire frequency range presented.

In future work the deviations in the verification measurements and for use cases have to be clarified and minimized. An advanced current distribution algorithm with a more exact current distribution replication and less needed current probe measurements will improve accuracy and diminish effort. Different kinds of coupling concepts and terminations for a segment during the TF generation have to be checked as well as multi wire bundle setups. Further, the method has to be adapted for average and quasi peak measurement results.

References

[1] I. E. Comission, "CISPR 25 Ed.3: Vehicles, boats and internal combustion engines - Radio disturbance characteristics - Limits and methods of measurement for the protection of on-board receivers," 2008.

[2] C. R. Paul, "A comparison of the contributions of common-mode and differential-mode currents in radiated emissions," *Electromagnetic Compatibility, IEEE Transactions on*, vol. 31, no. 2, pp. 189-193, May 1989.

[3] M. C. Di Piazza, A. Ragusa, G. Tine, and G. Vitale, "A model of electromagnetic radiated emissions for dual voltage automotive electrical systems," *Industrial Electronics, 2004 IEEE International Symposium on*, vol. 1, pp. 317-322, 2004.

[4] C. R. Paul, *Introduction to Electromagnetic Compatibility*. New York: John Wiley & Sons, Inc., 1992.

[5] D. Schneider, S. Tenbohlen, and W. Köhler, "Untersuchung von Vorhersagemethoden der Abstrahlung bei Komponententests nach CISPR 25," *EMV Düsseldorf 2012*, pp. 263-271, 2012.

[6] J. Jia, D. Rinas, and S. Frei, "Prediction of radiated fields from cable bundles based on current distribution measurements," *Electromagnetic Compatibility (EMC EUROPE), 2012 International Symposium on*, pp. 1-7, Sep. 2012.

[7] W. T. Smith and R. K. Frazier, "Prediction of anechoic chamber radiated emissions measurements through use of empirically-derived transfer functions and laboratory common-mode current measurements," *Electromagnetic Compatibility, 1998. 1998 IEEE International Symposium on*, vol. 1, pp. 387-392, 1998.

[8] D. Schneider, S. Tenbohlen, and W. Köhler, "Pre-compliance test method for radiated emissions of automotive components using scattering parameter transfer functions," *Electromagnetic Compatibility (EMC EUROPE), 2012 International Symposium on*, pp. 1-6, Sep. 2012.

[9] D. Schneider, M. Böttcher, S. Tenbohlen, and W. Köhler, "Pre-Compliance Test Method for Radiated Emissions with Multiple Segment Transfer Functions," *Electromagnetic Compatibility, 2013 IEEE International Symposium on*, Aug. 2013.

[10] R. Chundru, D. Pommerenke, and S. Chandra, "A new calibration method for current probes," *Electromagnetic Compatibility, 2004. EMC 2004. 2004 International Symposium on*, vol. 1, pp. 163-168, Aug. 2004.